Chinese Journal of Chemical Engineering 55 (2023) 192–201

Contents lists available at ScienceDirect

Chinese Journal of Chemical Engineering

journal homepage: www.elsevier.com/locate/CJChE

Full Length Article

Styrene epoxidation catalyzed by polyoxometalate/quaternary ammonium phase transfer catalysts: The effect of cation size and catalyst deactivation mechanism

Qiongna Xiao [1,2,3], Yuyan Jiang [1,2,3], Weiqiang Yuan [1,3], Jingjing Chen [1,2,3], Haohong Li [3,4], Huidong Zheng [1,2,3,*]

[1] College of Chemical Engineering, Fuzhou University, Fuzhou 350116, China
[2] Qingyuan Innovation Laboratory, Quanzhou 362801, China
[3] Engineering Research Center of Advanced Manufacturing Technology for Fine Chemicals, Fujian Province University, Fuzhou University, Fuzhou 350116, China
[4] College of Chemistry, Fuzhou University, Fuzhou 350116, China

ARTICLE INFO

Article history:
Received 15 December 2021
Received in revised form 25 April 2022
Accepted 26 April 2022
Available online 26 May 2022

Keywords:
Phosphotungstic acid phase-transfer catalyst
Styrene epoxidation
Catalyst deactivation mechanism
Cation size effect

ABSTRACT

Catalytic epoxidation of alkenes is an important type of organic reaction in chemical industry, and the deep insight into catalyst deactivation will help to develop new epoxidation process. In this work, series of quaternary ammoniums bearing different cationic sizes, *i.e.* $MTOA^+$ (methyltrioctylammonium, $[(C_8H_{17})_3CH_3N]^+$), $HTMA^+$(hexadecyltrimethylammonium, $[(C_{16}H_{33})(CH_3)_3N]^+$) and $DMDOA^+$ (dimethyldioctadecylammonium, $[(C_{18}H_{37})_2(CH_3)_2N]^+$) were incorporated with polyoxometalate (POM) anions to prepare phase transfer catalysts (PTCs), which were used in the styrene epoxidations. Among them, $(MTOA)_3PW_4O_{24}$ exhibits the best catalytic performance judged from the highest styrene conversion rate (52%) and styrene oxide selectivity (93%), during which the styrene epoxidation conditions were optimized. Meanwhile, the deactivation mechanism of this kind of PTCs was proposed firstly, *i.e.* in the case of low H_2O_2 content, the oxidant can only be used in the styrene epoxidation, in which the catalyst can transform into stable Keggin-type POM. But when the content of H_2O_2 is higher, the excess H_2O_2 can reactivate the Keggin-type POM into active $(PW_4O_{24})^{3-}$ anions, which can trigger the ring-opening polymerization of styrene oxide. Consequently, the catalyst is deactivated by adhered poly(styrene oxide) irreversibly, which was determined by NMR spectra. In this situation, the active moiety $\{PO_4[WO(O_2)_2]_4\}^{3-}$ in phase-transfer catalytic system can break into some unidentified species with low W/P ratio with the presence of epoxides. This work will be beneficial for the design of new PTCs in alkene epoxidation in fine chemical industry.

© 2022 The Chemical Industry and Engineering Society of China, and Chemical Industry Press Co., Ltd. All rights reserved.

1. Introduction

As an important kind of organic reaction, selective catalytic epoxidation has captured extensive interests for a long time, because the epoxides have exhibited a broad application range in chemical industry [1]. Among them, styrene oxide is an especially important intermediate for the synthesis of fine chemicals and pharmaceuticals [2]. For example, some aldehydes and ketones can be synthesized from styrene oxide *via* Meinwald rearrangement [3]. But up to now, in the industrial production, chlorohydrin method remains a dominant process, which bears some fatal shortcomings such as low yield, equipment corrosion, high energy consumption and environmental pollution [4]. The development of high efficiency and environment friendly epoxidation method is still desired. It's universally accepted that the hydrogen peroxide is an ideal oxidant in olefin epoxidation due to its economic viability and environmental feasibility [5]. The one-step epoxidation of styrene using H_2O_2 is a facile synthesis route, which could reduce side reactions and improve atomic utilization.

When concerning about the epoxidation catalysts, polyoxometalate (POM)-based catalysts have attracted special interests, because they can be feasibly modified at the molecular level to adjust the acid, base and/or redox properties [6]. So far, many kinds of POMs including lacunary polyoxotungstates, peroxotungstates, peroxomolybdates and transition metal-substituted POMs have exhibited high styrene oxide yields and efficient H_2O_2 utilization

* Corresponding author at: College of Chemical Engineering, Fuzhou University, Fuzhou 350116, China.
E-mail address: youngman@fzu.edu.cn (H. Zheng).

https://doi.org/10.1016/j.cjche.2022.04.024
1004-9541/© 2022 The Chemical Industry and Engineering Society of China, and Chemical Industry Press Co., Ltd. All rights reserved.

[7–18]. However, many problems still exist in these POM-based heterogeneous catalysts, including low mass transfer, excess amount of H_2O_2, longer reaction time [19,20]. The phase transfer catalysts (PTCs) can solve these disadvantages because they can combine the advantages of homogeneous catalysts (high activity, mass transfer elimination and good accessibility of substrates to catalytic active sites) and heterogeneous ones (facile separation and reusability) [21]. Up to now, series of quaternary ammoniums, including $[(n\text{-}C_4H_9)_4N]^+$, $[\pi\text{-}C_5H_5N(CH_2)_{15}CH_3]^+$, $[(C_8H_{17})_3NCH_3]^+$, $[C_{16}H_{33}N(CH_3)_3]^+$ and $[(C_{18}H_{37})_2(CH_3)_2N]^+$ have been adopted to modify the POMs in the olefin epoxidation [21,22]. Most of the reported olefin epoxidation with PTCs were executed in organic solvents, which could not meet the requirements of green chemistry. Therefore, it is significant to exploit new PTCs to achieve the organic solvent-free styrene epoxidation with equimolar H_2O_2. To our knowledge, the organic solvent-free olefin epoxidation can be achieved using saturated Na_2SO_4/H_2O_2 solution [9,23,24]. But for the electron-poor styrene, its organic solvent-free epoxidation using POM-based PTCs is still rare [25–29]. Moreover, the influence of cation size and the aggregation in the liquid–liquid interface on their catalytic activity is in its infancy [14]. Importantly, the deactivation mechanism of POM-based PTCs is still lack of the support of *in-situ* experimental data. In this work, series of POM-based PTCs containing different alkyl chain lengths were used in the organic solvent-free styrene epoxidations, whose deactivation mechanism was investigated by FT-IR and time-dependent ^{31}P NMR spectra. This work will provide theoretical guide for high efficiency epoxidation of electron-poor olefin in fine chemical industry.

2. Experimental

2.1. Reagents and characterization

All chemicals including $[(C_8H_{17})_3CH_3N]Cl$ (MTOA·Cl), $[(C_{16}H_{33})(CH_3)_3N]Cl$ (HTMA·Cl), $[(C_{18}H_{37})_2(CH_3)_2N]Cl$ (DMDOA·Cl), styrene, cyclohexene oxide, phosphoric acid (85%), $NaH_2PO_4{\cdot}12H_2O$, tungstic acid (H_2WO_4, 99%), hydrogen peroxide (30%), sodium thiosulfate anhydrous (Na_2SO_4, 99%), $Na_2WO_4{\cdot}2H_2O$, $H_3PW_{12}O_{40}{\cdot}xH_2O$ were obtained from commercial resource and used without further purification. Fourier transform infrared spectra (FTIR) were performed on the Thermo Scientific Nicolet iS50 spectrophotometer in the scanning range of 400–4000 cm^{-1}. *In-sit*u IR were executed on a Mettler-Toledo react-IR™ 15 analyzer. ^1H, ^{13}C and ^{31}P NMR spectra were recorded on a AVANCE NEO 600 (14.1 T/600 MHz) in $CDCl_3$. The concentrations in the reacting system were determined by a gas chromatograph (GC-2014C). And the qualitative identification of substrates, products and by-products were performed by the GC–MS (GC–MSQP2020 NX). TG analysis were conducted on STA449C/6/G thermal analyzer. The contents of P and W were measured by inductively coupled plasma emission spectrometer (ICP-MS-7700). The contents of C, H, N were measured by elemental analyzer (Vario EL cube, Elementar).

2.2. Catalysts preparation

$(MTOA)_3PW_4O_{24}$: The catalysts were synthesized according to literature method [9]. Firstly, in a three-neck flask, tungstic acid (H_2WO_4) (15.0 g, 60.0 mmol) and hydrogen peroxide (H_2O_2) (30%, 40 ml) was heated at 60 °C for 1 h, during which the bright yellow mixture turned into a pale-yellow solution. Then the hot solution was centrifuged at rate of 8000 $r{\cdot}min^{-1}$ for 5 min. Afterwards, 85% orthophosphoric acid (H_3PO_4) (1.72 g, 15.0 mmol) in distilled water (180 ml) was added into the obtained colorless supernatant and kept stirring of 10 min. 120 ml CH_2Cl_2 solution containing MTOA·Cl (21.21g, 52.5 mmol) was added dropwise in 15 min. The resultant emulsion was stirred vigorously for 20 min. Finally, the organic phase was separated to obtain raw product, which was dried in $NaSO_4$ and vacuum at 30−40 °C to remove CH_2Cl_2. Yellow paste catalyst can be obtained with yield of 70.0% (19.0 g). IR spectrum (KBr, cm^{-1}, Fig. S1(a)) 3387(s), 2927(s), 2859(s), 1646(w), 1554(w), 1474(s), 1375(m), 1028(s), 919(s), 839(s), 721(m), 595(w), 540(w). Elemental analysis: Cal. C 39.92%; H 7.25%; N 1.86%; O 17.01%; P 1.37%; W 32.58%; found: C 41.12%; H 7.14%; N 1.90%; O 16.57%; P 1.42%; W 31.88%.

$(HTMA)_3PW_4O_{24}$: The preparing procedure was similar with that of $(MTOA)_3PW_4O_{24}$, except ethanol was used to dissolve HTMA·Cl at 40 °C. Yield: 6.5 g, 66.5%. IR (KBr, cm^{-1}, Fig. S1(a), Supplementary Material): 3447(s), 2925(s), 2845(s), 1638(s), 1469(s), 1082(s), 1015(w), 952(s), 885(w), 864(w), 826(m), 716(m), 594 (w), 546(m).

$(DMDOA)_3PW_4O_{24}$: This catalyst was synthesized under the same conditions, except that excessive CH_2Cl_2 was added to dissolve DMDOA·Cl. Yield: 8.0 g, 69.7%. IR (KBr, cm^{-1}, Fig. S1(a)): 3434(s), 2928(s), 2853(s), 1642(s), 1468(s), 1380(w), 1090(s), 1024(w), 953(s), 886(w), 845(w), 717(m), 592(w), 551(m).

$(MTOA)_9PW_9O_{34}$: $Na_9[A\text{-}PW_9O_{34}]{\cdot}7H_2O$ was prepared according to literature method [30]. $Na_2WO_4{\cdot}2H_2O$ (1.2 g, 36.0 mmol) was dissolved in 15 ml ultra-pure water, and H_3PO_4 (0.4 ml, 6.0 mmol) was added to adjust the pH of 8.9–9.0. Afterwards, glacial acetic acid (2.25 ml, 0.4 mol) was dropped slowly, during which large amounts of white solids can be generated and the pH was in the range of (7.5 ± 0.3). The resultant suspension was stirred for another 1 h. In another flask, 50 ml CH_2Cl_2 solution containing MTOA·Cl (4.8 g, 12.0 mmol) was added dropwise into the above $[A\text{-}PW_9O_{34}]$ solution. The suspension was stirred for 1 h. Finally, the organic phase was separated to obtain raw product, which was dried in $NaSO_4$ and vacuum at 30−40 °C to remove CH_2Cl_2. Pale catalyst can be obtained with yield of 68.3% (8.5 g). IR (KBr, cm^{-1}, Fig. S1(b)): 3451(s), 2936(s), 2858(s), 1621(s), 1466(s), 1377(s), 1079(s), 1042(w), 948(s), 885(w), 889(w), 85(m), 822(s), 751(m), 595(w), 515(m).

$(MTOA)_7PW_{11}O_{39}$: $Na_7PW_{11}O_{39}{\cdot}13H_2O$ precursor was prepared using literature method [31]. $Na_2WO_4{\cdot}2H_2O$ (7.25 g, 22.0 mmol) and $NaH_2PO_4{\cdot}12H_2O$ (0.716 g, 2.0 mmol) were dissolved in 20 ml ultra-pure water, and the solution was heated to 80–90 °C with pH being adjusted to 4.8 by HNO_3. When about half of water was evaporated, 10 ml acetone was used to extract the product for three times. The product can be obtained by removal of acetone (7.42 g). The phase transfer catalyst $(MTOA)_7PW_{11}O_{39}$ was synthesized with the similar procedure of $(MTOA)_9PW_9O_{34}$. Yellow catalyst can be obtained with yield of 78.2% (7.8 g). IR (KBr, cm^{-1}, Fig. S1(b)): 3438(s), 2954(s), 2853(s), 1621(m), 1466(s), 1381(s), 1082(s), 1040(w), 956(s), 893(w), 860(w), 809(s), 755(m), 590 (w), 511(m).

$(MTOA)_3PW_{12}O_{40}$: The preparation of this catalyst was generally the same with that of $(MTOA)_7PW_{11}O_{39}$, except that $H_3PW_{12}O_{40}{\cdot}xH_2O$ was purchased from commercial source. Yield (78. 4%, 5.6 g). IR (KBr, cm^{-1}, Fig. S1(b)): 2954(s), 2925(s), 2852(s), 1482 (s), 1471(s), 1383(m), 1085(s), 977(s), 893(w), 819(s), 590(w), 519(m), 506(m).

2.3. Catalytic evaluation

In a 25 ml flask, styrene (30.0 mmol) and phase transfer catalysts (0.3 mmol) were mixed in oil bath and stirred at certain temperatures. When the catalysts have been dissolved completely and temperature reached to the setting value, 30% H_2O_2 (30.0 mmol) and Na_2SO_4 (9.0 mmol) were added dropwise. The product sample was extracted from reaction system at intervals, which was separated by centrifugation and toluene was used as internal standard.

After diluting with ethanol, gas chromatograph (GC-2014C) equipped with a flame ionization detector (FID) and a capillary column (InertCap5 30 m × 0.25 mm × 0.25 μm) was used to determine the concentrations of products. The injector, detector and oven temperatures were 250, 300 and 120 °C, respectively. The injection volume was 0.2 μl and the split ratio was set as 40 using N_2 as carrier gas.

The styrene conversion (X), epoxide selectivity (S) and turn over number (TON) are defined as follows:

$$X = \frac{M_{\text{styrene}^*} - M_{\text{styrene}}}{M_{\text{styrene}^*}} \times 100\%$$

$$S = \frac{M_{\text{epoxide}}}{M_{\text{styrene}^*} - M_{\text{styrene}}} \times 100\%$$

$$\text{TON} = \frac{M_{\text{epoxide}}}{M_{\text{w}}}$$

Here, M is molar number, w is tungsten atom, and the symbol * denotes the situation before reacting.

2.4. Catalyst recycling

After the styrene epoxidation was completed, the oil/water phase can be isolated by keeping it at room temperature. Then the oil phase was separated and small amount of *tert*-butylcatechol (TBC) was added to inhibit the styrene polymerization. The catalysts can be recycled by removal of substrates and products using distillation in vacuum. Na_2SO_4 can be recovered in water phase. The solution containing recovered catalysts, Na_2SO_4 and fresh 30% H_2O_2 will be used in the next epoxidation reaction.

3. Results and Discussion

3.1. Catalyst characterization

The fresh and recovered catalysts have been characterized with FT-IR and ^{31}P NMR spectra. The IR spectra of quaternary ammonium salts and their corresponding PTCs are shown in Fig. 1 and Fig. S1 (Supplementary Material). As revealed in Fig. S1, the characteristic vibrations of PTCs match well with their corresponding organic cations, implying that the quaternary ammoniums have been successfully incorporated with POM ions. In detail, the peaks at 3400 cm^{-1} and 1640 cm^{-1} are assigned to the stretching vibration of —OH and bending vibration of H—O—H in H_2O, suggesting the presence of water in catalysts. The characteristic vibrations of quaternary ammoniums can be detected in 2800–3000 cm^{-1} (stretching vibration of —CH_3), 1470/1380 cm^{-1} (symmetric/asymmetric stretching vibration of —CH_3) and 720 cm^{-1} (vibration of —CH_2) [32]. The characteristic peaks of POM locate at fingerprint regions. In detail, peaks among 1024–1125 cm^{-1} are the vibrations of P—$O_{tetrahedron}$ bonds, peaks at 920–960 cm^{-1} correspond to the vibrations of P—$O_{terminal}$ bonds, and those at 863, 884, 895 cm^{-1} are assigned to the ν(W—O_b—W) [22]. Specially, ν(O—O) can be found at about 842 cm^{-1}, and ν[W(O_2)] appears at 591, 543, 523 cm^{-1} [14]. The treatment of saturated Keggin-type $[PW_{12}O_{40}]^{3-}$ anion with H_2O_2 can lead to its degradation into some unidentified species, which have been further characterized by ^{31}P NMR spectrum (Fig. 1(b)). In $(MTOA)_3PW_4O_{24}$, three chemical shifts at 7.8, 3.6 and −7.9 can be monitored, and only one shift at 7.8 can be found in $(HTMA)_3PW_4O_{24}$, but two shifts at 7.8, −8.1 appear in $(DMDOA)_3PW_4O_{24}$. The species at δ = 3.6 in $(MTOA)_3PW_4O_{24}$ could be assigned to the $[(PO_4)\{WO(O_2)_2\}_4]^{3-}$ [33]. The peaks at δ = 7.8 are attributed to the polytungstophosphate species with low W/P ratio containing, and those at δ = −7.9/−8.1 may be assigned to polytungstophosphate species with high W/P ratio [34]. Furthermore, only one chemical shift can be detected in $(MTOA)_9PW_9O_{34}$ (δ = −9.8) and $(MTOA)_3PW_{12}O_{40}$ (δ = −14.6), which are consistent with literature [35]. But two peaks at δ = −9.8, −12.1 can be observed in $(MTOA)_7PW_{11}O_{39}$, hinting that the co-existence of $(PW_9O_{34})^{9-}$ specie. During our synthesis processes, the structures of POM can be controlled by adjusting the pH values, during which different POM anions $[(PW_4O_{24})^{3-}$, $(PW_9O_{34})^{9-}$, $(PW_{11}O_{39})^{7-}]$ can be generated [30,31]. These catalysts can exhibit different catalytic epoxidation performances, which will be discussed in the following section.

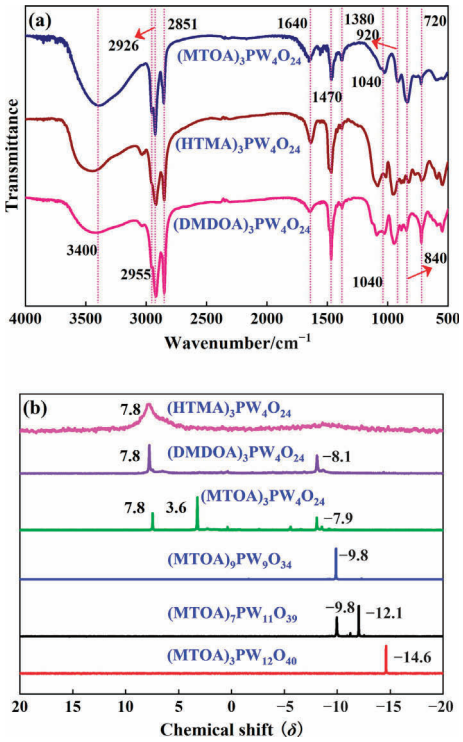

Fig. 1. (a) IR spectra of three $PW_4O_{24}^{3-}$-based phase transfer catalysts; (b) ^{31}P NMR spectra of six phase transfer catalysts.

3.2. Styrene epoxidation catalyzed by structurally relative PTCs

Compared with the extensively studied olefins such as chloropropene and cyclohexene, the epoxidation of electron-poor styrene is still lack of deep insight, especially its green solvent-free synthesis. In this section, by introducing Na_2SO_4 into in the liquid–liquid two-phase reaction of styrene, the effect of Na_2SO_4 and catalyst structures (cation sizes, POM ion species and the aggregation modes) were disclosed.

The effect of Na_2SO_4 on the epoxidation performance was evaluated firstly. As revealed in Table 1, under the organic solvent-free condition without Na_2SO_4, the styrene conversion is 88% after reacting for 1 h, but the styrene oxide selectivity is lower than 3%. The main products are 1-phenyl-1,2-ethanediol accompanied by benzaldehyde, benzoic acid and 2-hydroxy acetophenone. With the presence 9 mmol Na_2SO_4 with reacting time of 1 h, the styrene conversion is 53%, and the styrene oxide selectivity can reach to 80%, which is considerable. The better epoxidation performance could be explained as the salting-out effect, which can decrease the amount of styrene oxide in water and inhibit its hydrolysis [36]. This result has also been observed in the terpene epoxidation [9,24]. But the salting-out effect can also decrease the mass trans-

Table 1
The effect of sodium sulfate on the styrene epoxidation under solvent-free conditions

	Na_2SO_4/ mmol	Temperature/°C	Reaction time/h	Styrene conversion/%	Styrene oxide selectivity/%
1	9	50	1	53	80
2	0	50	1	88	<3

Note: Reaction conditions is styrene: 30 mmol, 30% H_2O_2: 30 mmol.

fer rate in liquid–liquid interface, resulting in lower styrene conversion [37]. Secondly, the effect of quaternary ammoniums on epoxidation was investigated. Herein, three structurally relative quaternary ammoniums were used to prepare $A_3PW_4O_{24}$ PTCs (A = $MTOA^+$, $HTMA^+$, $DMDOA^+$), which were used in the styrene epoxidation. Judged from Fig. S2, $(MTOA)_3PW_4O_{24}$ exhibits the best catalysis performance with the highest conversion and selectivity, and the order is $(MTOA)_3PW_4O_{24}$> $(DMDOA)_3PW_4O_{24}$ > $(HTMA)_3PW_4O_{24}$. This order is consistent with their solubility in nonpolar solvent. The better its lipo-solubility is, the higher catalytic activity can be achieved [14]. Furthermore, the reaction rate will be gradually lowered with elongating reacting time, which is led by catalyst deactivation. Thirdly, series of POM anions were considered in styrene epoxidation based on the above screening of cations, *i.e.* $(MTOA)_9PW_9O_{34}$ (tri-defective Keggin), $(MTOA)_7PW_{11}O_{39}$ (mono-defective Keggin) and $(MTOA)_3PW_{12}O_{40}$ (saturated Keggin). As indicated by Fig. S3, the highest conversion can also be observed in $(MTOA)_3PW_4O_{24}$ system, but the selectivity is high as 88% within 1 h. With the elongation of reacting time, the selectivity will decrease clearly, which is led by the side reactions such as hydrolysis and isomerization [38]. In all, for electron-poor styrene, the catalytic activity is dominated by $[(PO_4)\{WO(O_2)_2\}_4]^{3-}$ specie, which leads to the active order of $(MTOA)_3PW_4O_{24}$ > $(MTOA)_7PW_{11}O_{39}$ > $(MTOA)_9PW_9O_{34}$ > $(MTOA)_3PW_{12}O_{40}$ [33]. Therefore, $(MTOA)_3PW_4O_{24}$ is selected in the following organic solvent-free styrene epoxidation.

3.3. Styrene epoxidation catalyzed by $(MTOA)_3PW_4O_{24}$

The catalytic performance of $(MTOA)_3PW_4O_{24}$ for the styrene epoxidation was optimized in terms of reacting temperature, Na_2SO_4, catalyst and oxidant amounts. Firstly, the temperature was screened judged from the conversion and epoxide selectivity (Fig. 2(a)), during which epoxidation reactions were carried out in temperature range of 20–60 °C. The highest conversion rate can be achieved when the reaction temperature is 30 °C, which might be led by the powerful exothermal nature of epoxidation. Besides, the best selectivity can also be obtained at 30 °C. The considerable conversion (63%) and epoxide selectivity (88%) can be given when the reacting time is 2 h. Secondly, the effect of the catalyst content was investigated (Fig. 2(b)), in which 1/50, 1/100, 1/150 and 1/200 have been considered. When the catalyst contents increase from 1/200 to 1/50, the conversion rates are improved from 39% to 93%. The selectivity being higher than 95% can be obtained when the catalyst contents are among 1/200–1/100, which will decrease gradually with reacting time. But much lower selectivity can be observed when the catalyst content is 1/50, in which many side-reactions such as isomerization and hydrolysis have happened. Therefore, the optimal catalyst content is set as 1/100. Thirdly, Na_2SO_4 is necessary for the organic solvent-free styrene epoxidation, whose content must be explored. Herein, 3, 6 and 9 mmol Na_2SO_4 have been used, which are revealed in Fig. 2(c). Interestingly, both the conversion and selectivity increase with the Na_2SO_4 amount, based on which the 9 mmol Na_2SO_4 is adopted in the epoxidation. But the conversion is lower than that without Na_2SO_4, which is led by the decrease of phase contact

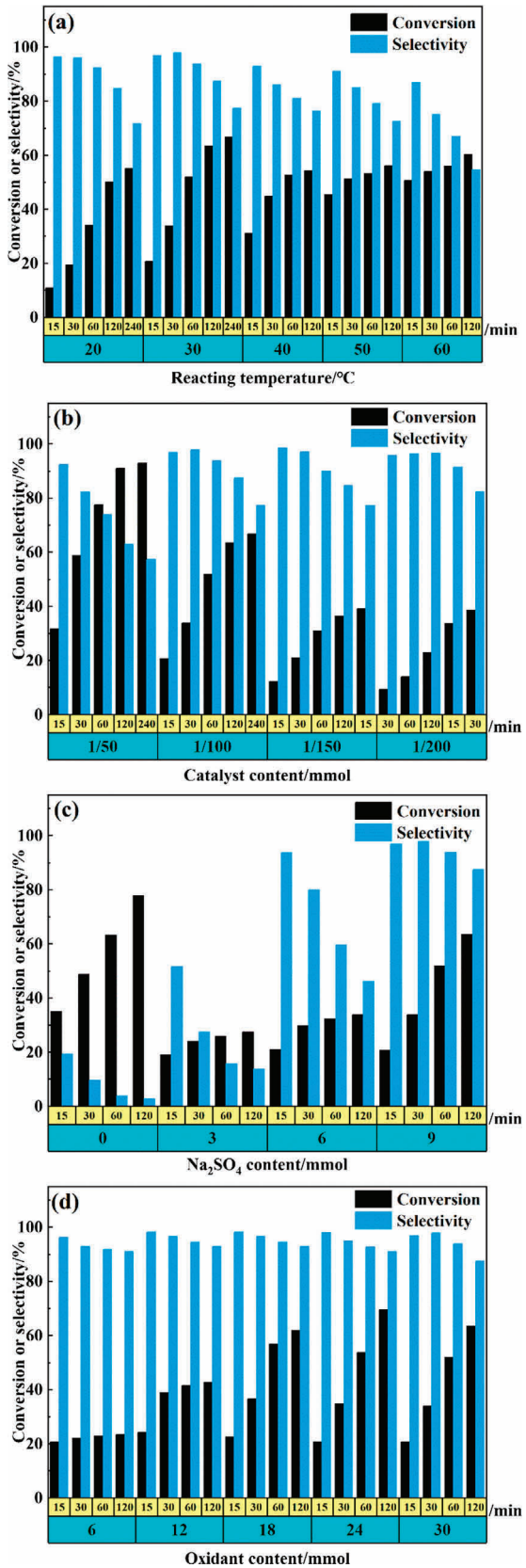

Fig. 2. Optimization for solvent-free styrene epoxidation: (a) reacting temperature (reaction conditions: styrene 30 mmol, $(MTOA)_3PW_4O_{24}$ 0.3 mmol, 30% H_2O_2 30 mmol, Na_2SO_4 9 mmol; (b) catalyst content (reaction conditions: 30 °C, styrene 30 mmol, 30% H_2O_2 30 mmol, Na_2SO_4 9 mmol); (c) Na_2SO_4 content (reaction conditions: 30 °C, styrene 30 mmol, $(MTOA)_3PW_4O_{24}$ 0.3 mmol, 30% H_2O_2 30 mmol); (d) oxidant content (reaction conditions: 30 °C, styrene 30 mmol, $(MTOA)_3PW_4O_{24}$ 0.3 mmol, molar ratio of Na_2SO_4 and H_2O_2 3:10).

between styrene-containing oil phase and H_2O_2-containing water phase [39]. But many by-products will generate in the situation without Na_2SO_4. Previous work has pointed out that the molar ratio of Na_2SO_4 to H_2O_2 higher than 0.3 could not promote the epoxidation because of bad solubility in oil phase [23]. Finally, we then pay attention to the effect of oxidant amount on the epoxidation performance. The concentration of hydrogen peroxide is subtle for epoxidation, because inappropriate amounts will lead to oxidation insufficiency or side reactions [40]. Herein, five H_2O_2 amounts (6, 12, 18, 24 and 30 mmol,) were considered (Fig. 2 (d)). When the H_2O_2 content is lower than 12 mmol, the conversion rate is lower than 40%, and the other three contents exhibit the similar conversion rates (65%–70%). But the selectivity demonstrates the contrary trend, *i.e.* higher H_2O_2 content can result in lower selectivity, which might be led by the catalyst deactivation with the co-existence of styrene oxide and excess H_2O_2. In this work, the H_2O_2 amount of 15 mmol is adopted, based on which considerable conversions and selectivity can be obtained. In all, the optimal conditions of organic solvent-free styrene epoxidation catalyzed by $(MTOA)_3PW_4O_{24}$ can be summarized as follows: 30 °C, catalyst content 1% (mol), 9 mmol Na_2SO_4 and 15 mmol H_2O_2, reacting time 1 h. And the catalytic performance of $(MTOA)_3PW_4O_{24}$ under this condition is better than other styrene epoxidations using other POMs-bearing catalysts (Table 2) [28,41–43].

3.4. The recovery of catalyst and side reaction

The recovery and reusability of catalyst are important for industrial production. In this work, the $(MTOA)_3PW_4O_{24}$ catalyst was recovered by distillation in vacuum, which was used in the next three epoxidation cycles (Table 3). During this process, only species with relatively low boiling points can be removed. Therefore, the mass of recovered catalysts is larger than the initial amount, which is caused by the polymer adhesion stemming from the ring-opening polymerization of epoxide. The continuous accumulation of high boiling point materials in the catalyst cycle is inevitable. The problem might be solved by appropriate solvents, which is worth investigating in the further study. Clearly, the catalytic activities of recovered catalysts decrease gradually. In the second cycle, the conversions and selectivity are lowered slightly (45% and 94% respectively), but they are decreased sharply in third (32% and 76%) and fourth cycles (15% and 75%). The accumulative TON of four cycles is 31.4 mol·mol^{-1}, which is much higher than the case using equal catalyst content and H_2O_2 (13.9 mol·mol^{-1}). Thus, the lower H_2O_2 content can heighten the catalyst stability.

In order to clarify the catalyst deactivation process, IR, ^{31}P NMR and ICP-MS were conducted on recovered samples. In the IR spectra (Fig. 3(a)), the ν(O—O) peak at 840 cm^{-1} for fresh catalyst splits into two peaks at 890 cm^{-1} (ν(W—O_b—W)) and 820 cm^{-1} (ν(W—O_c—W)) for recovered one, suggesting the consuming of active oxygens. The characteristic vibration of ν(P—O_a) (1000–1100 cm^{-1}) was broadened with recovering cycles, which is led by the overlap of ν(C—O) in poly(styrene oxide). Besides, the characteristic peaks of at 1717 cm^{-1}, 1200–1300 cm^{-1} verify again the formation of poly(styrene oxide) [44]. The weak peaks in 3089–3029 cm^{-1}, 1950–1820 cm^{-1} and strong peaks at 758, 700 cm^{-1} can be assigned to the vibrations of benzene. Thus the IR spectra imply the formation of poly(styrene oxide), which is accumulated with the recovered cycles. Besides, As indicated by ^{31}P NMR spectra, the defective Keggin anions (PW_{11}: δ = −12.1) are dominant in the firstly recovered catalyst, and only small part of catalyst has

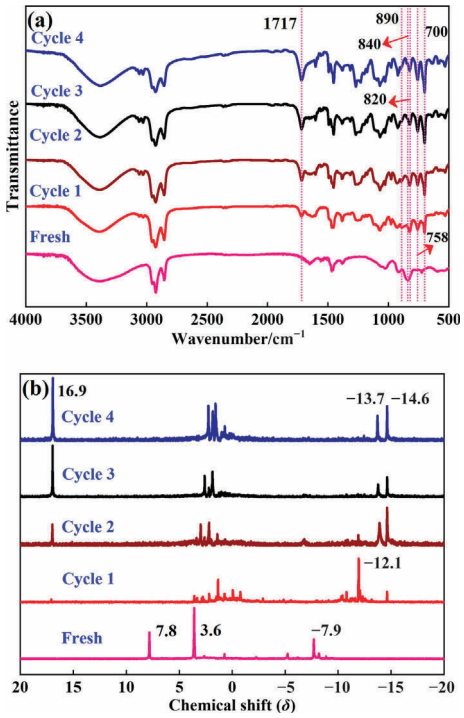

Fig. 3. IR spectra (a) and ^{31}P NMR (b) of recovered catalyst with four cycles.

Table 2
Epoxidation of styrene in various catalysts

Catalyst	Oxidant	Solvent	Temperature/°C	Reaction time/h	Styrene conversion/%	Styrene oxide selectivity/%	Ref.
$(MTOA)_3PW_4O_{24}$	H_2O_2	/	30	1	52	93	This work
$Cs_7[PW_{10}Cu_2(H_2O)O_{38}]$	TBHP	/	/	/	52	78	[28]
$Na_3K_4[BW_{12}O_{40} \subset H_4Mo_{72}Fe_{30}O_{254}(CH_3COO)_{16}(H_2O)_{96}]$	H_2O_2	Ethanol	75	3.5	85	89	[41]
$C_{48}H_{44}Cu_4N_9O_{71.5}P_2W_{18}$	TBHP	Acetonitrile	80	/	85	65	[42]
$[Co_3(bpdo)_6(H_2O)_4Cl_2][SiW_{12}O_{40}]\cdot H_2O$	H_2O_2	Acetonitrile	60	4	58	90	[43]

Table 3
The performances of recovered catalyst

Cycle	Catalyst content/g	Recovered amount/g	Reacting time/h	Styrene conversion/%	Styrene oxide selectivity/%	TON/mol·mol^{-1}
1	0.7082	0.7517	2	50	95	11.9
2	/	0.8366	3	45	94	22.5
3	/	0.9832	3	32	76	28.5
4	/	1.0036	3	15	75	31.4

Note: Reaction conditions is 30 °C, styrene 30 mmol, 30% H_2O_2: 15 mmol, Na_2SO_4 4.5 mmol.

deactivated (Fig. 3(b)). In the second and third recovered cycles, the defective Keggin anions became non-defective gradually (PW_{12}: δ = −14.6), and some deactivated species appearing in 3.0–1.3 might be led by the surplus H_2O_2 and styrene oxide. Specially, the new species appearing in 16.9 might correspond to the saturated POM anions. In its fourth cycle, further deactivation has occurred, corresponding its sharp decreasing of conversions and selectivity.

So as to further validate the generation of ring-opening polymerization, an addition experiment using styrene oxide as reactant and $(MTOA)_3PW_4O_{24}$ as catalyst was executed. 0.3 mmol catalyst was dissolved in 30 mmol styrene oxide, which was heated to 50 °C. Then 30 mmol 30% H_2O_2 aqueous solution containing 9 mmol Na_2SO_4 was added. The mixture was kept stirring for 1 h. The product was determined by IR and NMR (Fig. S4). The characteristic peaks of ν(C—O) (1070 cm^{-1}) and benzene (3085, 3062, 3031, 1957, 1892, 1811, 1603, 1493, 700 cm^{-1}) are consistent with those of poly(styrene oxide) in literature (Fig. S4(a)) [44]. Other peaks are the vibrations of POM, suggesting the co-existence of poly(styrene oxide) and POM. In the ^1H NMR spectrum (Fig. S4 (b)), the chemical shifts in δ = 7.1–7.5 indicate the presence of benzene, and those in δ = 3.4–3.9 and 4.8–4.9 can be assigned to the hydrogen atoms of —O—CH_2 and —O—CH fragments in polymer chain, respectively [44,45]. Besides, the chemical shifts in δ = 1.2–1.4 and 0.91–0.93 can be attributed to the quaternary ammonium salts. The ^{13}C NMR spectrum is in agreement with the ^1H NMR, in which the C on benzene (δ = 125–130, 141.2), C atoms of —O—CH_2 on polymer chain (δ = 74.8), C atoms of —O—CH on polymer chain (δ = 77–78), and C on quaternary ammonium (δ = 14.2, 22.6, 22.8, 26.4, 29.2, 31.8) can be observed (Fig. S4(c)). These information suggests the presence of poly(styrene oxide) due to ring-opening polymerization of styrene oxide.

3.5. Catalyst deactivation factors

3.5.1. The effect of temperature

According to the TG-DTG analysis, the $(MTOA)_3PW_4O_{24}$ catalyst can be stable up to 80 °C (Fig. S5(a)), therefore, the catalytic performances using catalysts treated at 60 and 80 °C were considered (Table 4). Compared with the un-treated catalyst, the catalytic performances of thermally-treated ones only decrease slightly, and the small amount of weight loss might be induced by lose of active oxygen. IR and ^{31}P NMR spectra were conducted on the thermally-treated catalysts. As shown by IR spectra (Fig. S5(b)), the sample treated at 60 °C changes little, except that the weakening of ν (O—O) vibration at 840 cm^{-1}. But this peak disappears when heated at 80 °C for 12 h, and two new peaks at 890, 820 cm^{-1} appear, hinting the loss of active oxygen and the formation of stable W—O—W bonds. This trend was also verified by ^{31}P NMR spectra (Fig. 4(a)), the chemical environment of P at 60 °C is generally the same with un-treated one. However, after treating at 80 °C for 12 h, the chemical shifts move towards low filed, corresponding

Table 4
Catalytic performance evaluation of thermally-treated catalysts

	Treated methods(12 h)	Fresh catalyst content/g	Treated catalyst amount/g	Styrene conversion/%	Styrene oxide selectivity/%
1	/	0.7046	/	50	92
2	60 °C	0.7104	0.6893	49	92
3	80 °C	0.7105	0.6649	47	88

Note: Reaction conditions is 50 °C, styrene 30 mmol, $(MTOA)_3PW_4O_{24}$ 0.3 mmol, 30% H_2O_2 15 mmol, Na_2SO_4 4.5 mmol, reacting time 30 min.

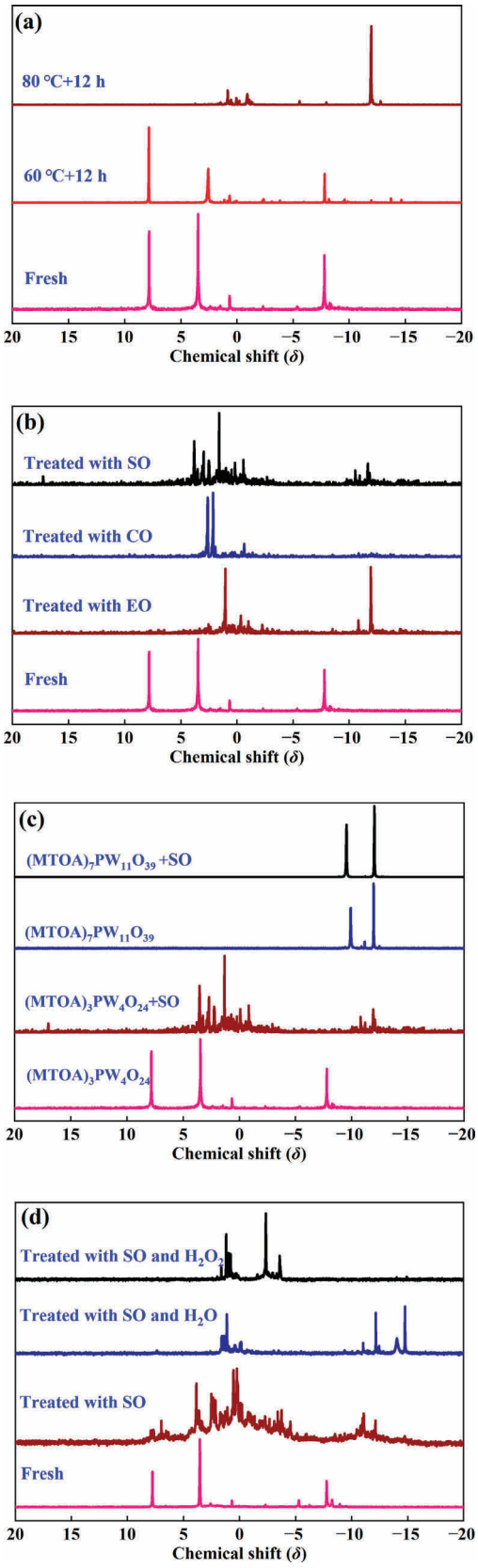

Fig. 4. ^{31}P NMR: (a) thermally treated samples; (b) epoxide-treated catalysts; (c) $(MTOA)_3PW_4O_{24}$ and $(MTOA)_7PW_{11}O_{39}$ before and after treated with SO; (d) $(MTOA)_3PW_4O_{24}$ co-treated with H_2O/H_2O_2 and SO.

to the formation of saturated Keggin-type POM. Hence, the active $[(PO_4)\{WO(O_2)_2\}_4]^{3-}$ trends to convert into stable Keggin-type anion at the temperature being higher than 80 °C. But according to literature [33], the stable Keggin-type anion can still be re-activated by H_2O_2. Generally, the effect of temperature on catalyst deactivation is not dominant.

3.5.2. The effect of epoxide

According to the experimental fact, the catalyst deactivation is accompanied by the generation of epoxide. Therefore, the effect of epoxide should be considered by the following measurement: 0.3 mmol catalyst was dissolved in 30 mmol epoxide (styrene oxide (SO), 1,2-epoxyoctane (EO), cyclohexene oxide (CO)) and kept stirring at 50 °C for 1 h, the recovered catalyst by removing styrene epoxide was used in the performance evaluation. As depicted by Table 5, the presence of epoxides can lower its catalytic performance, in which the highest deactivation can be found in CO-containing one. Comparably, only slight decrease can be observed in the EO-containing one (about 2% decrease in conversion and selectivity). As shown by IR spectra (Fig. S5(c)), the vibration peaks of EO-treated catalyst change little, in which only the disappearance of ν(O—O) (840 cm^{-1}) and appearance of ν(W—O—W) (880, 820 cm^{-1}) have occurred. But in the SO-treated catalyst, the characteristic vibrations of benzene (3085, 3061, 3030, 1603, 700 cm^{-1}) and ν(C—O—C) (1070 cm^{-1}) appear, corresponding to the ring-opening polymerization of SO. The weight increase of catalyst can be assigned to the formation of poly(styrene oxide) polymer. Besides, the appearance of ν(C=O) (1717 cm^{-1}) and ν(C—O) (1273 cm^{-1}) could be ascribed to the generation of benzoas groups due to the degradation of poly(styrene oxide) [44]. Similar behavior can be observed in the CO-treated catalyst, in which the characteristic vibrations of poly(cyclohexene oxide) can be found (1076 cm^{-1}: ν(C—O—C), 2930, 2857, 760 cm^{-1}: ν_{as}(—CH_2), ν_s ((—CH_2), δ(—CH)) [46]. Compared with the ^{31}P NMR spectra of fresh catalyst (Fig. 4(b)), the main differences lie in their movement to −1.0–3.6 (low W/P species) and −12.0 to − 10.0 (defective Keggin with high-polymerization degree, *i.e.* PW_9 and PW_{11}). The EO-treated catalyst can present the highest PW_{11} content, resulting in its good catalytic performance. But in the CO-treated one, no such active species can be detected, leading to its bad catalytic performance. In all, epoxides can lead to the catalyst deactivation by their ring-opening polymerizations, and the deactivated degree is relative to the kinds of epoxides.

3.5.3. The effect of catalyst component

As suggested by Section 3.2, $(MTOA)_3PW_4O_{24}$ exhibits the best catalytic performance in styrene epoxidation. While their tolerance to styrene oxide is still unclear, thus the catalytic performances of SO-treated $(MTOA)_3PW_4O_{24}$ and $(MTOA)_7PW_{11}O_{39}$ were evaluated (Table 6). As shown by Table 6, the styrene conversion reduced from 50% to 46% and styrene epoxide selectivity decreased from 92% to 85% when $(MTOA)_3PW_4O_{24}$ was treated with styrene oxide. But the same treatment on $(MTOA)_7PW_{11}O_{39}$ could not change the conversion and selectivity. In other words, upon styrene oxide treatment, the activity of $(MTOA)_3PW_4O_{24}$ decreases clearly, but that of $(MTOA)_7PW_{11}O_{39}$ can be maintained. As indicated by ^{31}P NMR (Fig. 4(c)), after mixing with SO, the chemical shifts of $(MTOA)_3PW_4O_{24}$ move to the range of δ = 3.8 to −1.0, hinting its deactivation due to loss of active oxygen. But those of $(MTOA)_7PW_{11}O_{39}$ change little. IR spectra also support this conclusion (Fig. S5(d)), in the SO-treated $(MTOA)_3PW_4O_{24}$, the characteristic vibrations of poly(styrene oxide) can be observed (3085, 3061, 3030, 1716, 1603, 1273, 1070, 700 cm^{-1}), but no such behavior can be found in SO-treated $(MTOA)_7PW_{11}O_{39}$. Therefore, $(MTOA)_3PW_4O_{24}$ with lower polymerization degree is prone to deactivate, but $(MTOA)_7PW_{11}O_{39}$ can exhibit better tolerance to SO.

3.5.4. The effect of H_2O_2

The presence of H_2O_2 can give rise to the ring-open polymerization of epoxide, therefore, the catalytic performance of catalyst co-treated with H_2O/H_2O_2 and SO were executed (Table 7). Compared with the systems without H_2O_2 (entries 1–3), the performance of

Table 5
Catalytic performance evaluation of epoxide-treated catalysts

	Treated method (50 °C for 1 h)	Fresh catalyst content/g	Treated catalyst amount/g	Styrene conversion/%	Styrene epoxide selectivity/%
1	/	0.7046	/	50	92
2	SO	0.7082	0.8541	46	85
3	EO	0.7082	0.7634	48	90
4	CO	0.7051	0.9514	45	75

Note: Reacting conditions is 50 °C, styrene 30 mmol, treated $(MTOA)_3PW_4O_{24}$ 0.3 mmol, 30% H_2O_2 15 mmol, Na_2SO_4 4.5 mmol, reacting time 30 min.

Table 6
Catalytic performance of different catalysts before and after styrene oxide treatment

	Catalyst	Treated methods (50 °C for 1 h)	Styrene conversion/%	Styrene oxide selectivity/%
1	$(MTOA)_3PW_4O_{24}$	/	50	92
		SO	46	85
2	$(MTOA)_7PW_{11}O_{39}$	/	42	86
		SO	43	86

Note: Reaction conditions is 50 °C, styrene 30 mmol, treated catalyst 0.3 mmol, 30% H_2O_2 15 mmol, Na_2SO_4 4.5 mmol, reacting time 30 min.

Table 7
Catalytic performance of catalysts co-treated by H_2O/H_2O_2 and styrene oxide

	Treated methods (50 °C for 1 h)	Fresh catalyst content/g	Treated catalyst amount/g	Styrene conversion/%	Styrene oxide selectivity/%
1	/	0.7046	/	50	92
2	SO	0.7082	0.8541	46	85
3	SO + H_2O/Na_2SO_4	0.7121	0.8614	15	86
4	SO + H_2O_2/ Na_2SO_4	0.7131	3.2776	4	48

Note: Reaction conditions is 50 °C, styrene 30 mmol, treated $(MTOA)_3PW_4O_{24}$ 0.3 mmol, 30% H_2O_2 15 mmol, Na_2SO_4 4.5 mmol, reacting time 30 min.

H_2O_2-containing one decreases sharply (entry 4), so conclusion could be drawn that H_2O_2 can accelerate the deactivation process, and the weight gain of recovered catalyst can be ascribed to the polymerization of SO. As revealed by ^{31}P NMR, more Keggin-type POM with higher polymerized degree can be monitored after treating with SO/H_2O (PW_{11}: δ = −12.1; PW_{12}: δ = −12.6, Fig. 4(d)), and the species with low W/P ratio decrease (δ = 1.7 to −0.3, PO_4^{3-}: δ = 1.3). This result proves again the un-stability of $(PW_4O_{24})^{3-}$ anion in water [33]. The further treatment of H_2O_2 can promote the movement towards lower filed (δ = −2.4 and −3.6), which might be led by the deactivation of SO on re-activated catalyst. The formation of poly(styrene oxide) can also be supported by IR spectra, in which the characteristic vibrations (3085, 3061, 3030, 1957, 1888, 1814, 1716, 1603, 1493, 1273, 1230, 1070, 758 and 700 cm^{-1}) can be detected (Fig. S5(e)). Therefore, under the co-existence of H_2O_2 and SO, some active POM anions undergo irreversible deactivation, and the rest Keggin-type POM can be activated by H_2O_2 to generate active $(PW_4O_{24})^{3-}$ anions, which can further be de-activated by ring-opening polymerization of epoxide. Therefore, the excessive H_2O_2 is the main reason for the catalyst deactivation. This new deactivation mechanism is beneficial for the development new epoxidation process.

3.6. Catalytic and deactivated mechanisms

The catalytic mechanism was proposed based on the *in-situ* IR. As shown by lines (2)–(4) in Fig. 5(a), after mixing the catalyst with styrene at 50 °C for 10, 20 and 30 min, the ν(O—O) band at 846 cm^{-1} in the fresh catalyst vanish gradually and three new vibrations of ν(W—O_b—W) (878 cm^{-1}), ν(W—O_c—W) (822 cm^{-1}), ν(C—H) of SO (757 cm^{-1}) appear, which corresponds to the transfer of active oxygen on the [W(O_2)] three-membered ring species to styrene to generate a concurrent W—O_b—W bond. As revealed by lines (5)–(7) in Fig. 5(b), after adding the hydrogen peroxide (0.1 eq., based on styrene) into the above solution, the band of ν(O—O) can appear again, which is accompanied by the vanishment of ν(W—O_c—W), which could be attributed to the re-generation of active structural unit containing [$W_2O_2(\mu\text{-}O_2)_2(O_2)_2$]. After elongating the reacting time for 10 min, the band of ν(O—O) disappears again, at the meantime, two bands ν(W—O_b—W) and ν(W—O_c—W) (at 822 and 878 cm^{-1}) can appear. And the ν(C—H) is enhanced, implying the increasing content of SO. Based on the above fact, the POM catalyst can act as mediator, which transfers the active oxygen from H_2O_2 to styrene oxide in the oil/water interface [15].

In order to further verify the above experimental results, *in-situ* ^{31}P NMR measurements on $(MTOA)_3PW_4O_{24}$ were conducted as follows: 0.3 mmol catalyst was dissolved in 30 mmol styrene and heated to 50 °C, then Na_2SO_4-containing 30% H_2O_2 was added, the oil phase was extracted at certain intervals for ^{31}P NMR analysis. As shown in Fig. 5(c), when 15 mmol H_2O_2 was used as oxidant, $(PW_4O_{24})^{3-}$ anions (δ = 3.6) can transform into Keggin-type POM (lower field), during which only small amount of deactivated species can be found (δ = −1.0–2.5). When using 30 mmol H_2O_2, its transformation to saturated Keggin-type POM can also be found, but the deactivated species locating at δ = 2.9, 1.9 and 0.2 are dominant after reacting for 30 min, which is the same with the SO-treated situation (Fig. 5(d)). Therefore, the following catalytic and deactivation mechanism can be proposed (Fig. 5(e)): when the oxidant content is low, it can only be used in the styrene epoxidation and the concentration of styrene oxide is relatively low. In this case, the catalyst can transform into stable Keggin-type POM, which is stable in styrene oxide. But when the dose of H_2O_2 is high, the excess H_2O_2 can re-activate the Keggin-type POM into active $(PW_4O_{24})^{3-}$ anions, which can trigger the ring-opening polymerization of styrene oxide. Consequently, the generation of some unidentified species with low W/P ratio accompanied by polymer

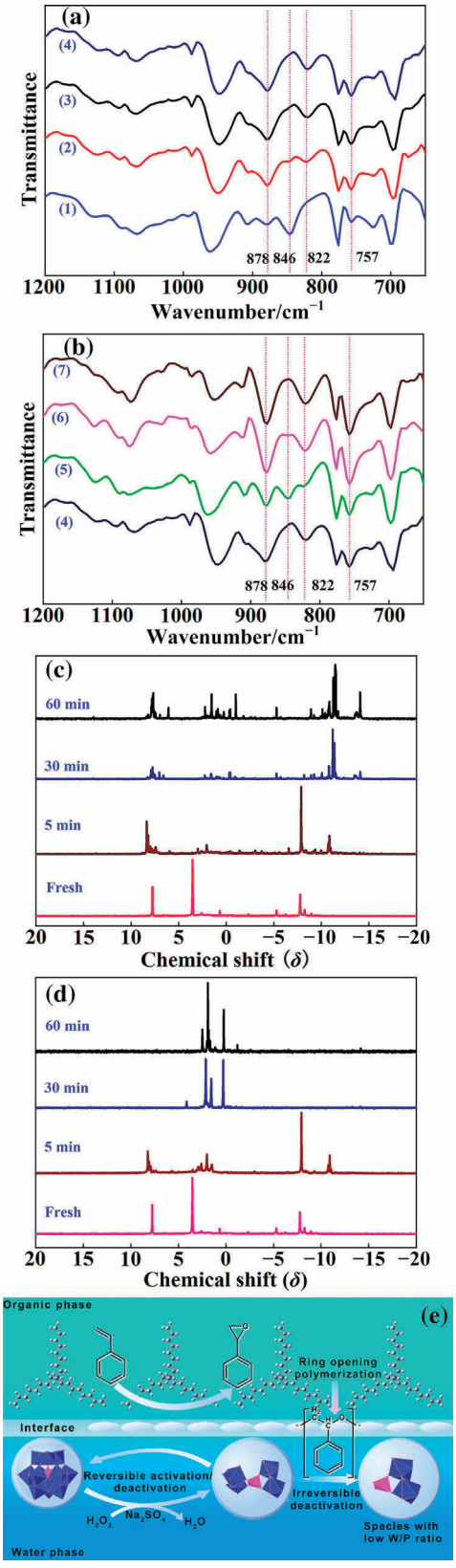

Fig. 5. *In-situ* IR spectra of the catalyst at different reacting time (50 °C, styrene 30 mmol, catalyst 0.3 mmol). (a) Line (1): fresh catalyst in styrene, line (2): reacting for 10 min, line (3): reacting for 20 min, line (4): reacting for 30 min. (b) Line (5): addition of 3 mmol H_2O_2 after reacting for 30 min, line (6): additional 5 min after addition of 3 mmol H_2O_2, line (7): additional 10 min after addition of 3 mmol H_2O_2. Time-dependent ^{31}P NMR spectra of $(MTOA)_3PW_4O_{24}$: (c) 15 mmol H_2O_2. (d) 30 mmol H_2O_2. (e) Catalytic and deactivation mechanism in liquid–liquid reaction using H_2O_2.

adhesion have occurred during the irreversible catalyst deactivation. The work about regeneration of deactivated catalyst is significant, which is still ongoing.

4. Conclusions

In summary, three polyoxometalate (POM)/quaternary ammonium phase transfer catalysts (PTC) possessing different cation sizes were used in the organic solvent-free styrene epoxidations, in which $(MTOA)_3PW_4O_{24}$ exhibits the best catalytic activity with styrene conversion rate (52%) and styrene oxide selectivity (93%). Furthermore, the epoxidation conditions catalyzed by $(MTOA)_3$-PW_4O_{24} were optimized. Meanwhile, the deactivation mechanism of PTC was investigated by considering the effects of temperature, epoxide, catalyst type and hydrogen peroxide. The deactivation mechanism of this kind of PTCs was proposed firstly: in the case of low H_2O_2 content, the active $\{PO_4[WO(O_2)_2]_4\}^{3-}$ can transform into stable Keggin-type POM; but in the situation of high H_2O_2 content, the $(PW_4O_{24})^{3-}$ species re-activated by excess H_2O_2 can trigger the ring-opening polymerization of styrene oxide to result in deactivation, during which the catalyst is broken into some unidentified species with low W/P ratio by adhered poly(styrene oxide). This work will be beneficial for the design of new PTC in alkene epoxidation in fine chemical industry.

Data Availability

Data will be made available on request.

Declaration of Competing Interest

The authors declare that they have no known competing financial interests or personal relationships that could have appeared to influence the work reported in this paper.

Acknowledgements

This study was financial supported by the National Natural Science Foundation of China (22078065), Key Program of Qingyuan Innovation Laboratory (00221001) and Quanzhou City Science & Technology Program of China (2020C008R).

Supplementary Material

Supplementary data to this article can be found online at https://doi.org/10.1016/j.cjche.2022.04.024.

References

[1] W.J. Yan, Y.H. Wu, X. Feng, C.H. Yang, X. Jin, J. Shen, Selective propylene epoxidation in liquid phase using highly dispersed Nb catalysts incorporated in mesoporous silicates, *Chin. J. Chem. Eng.* 26 (6) (2018) 1278–1284.
[2] M.S. Batra, R. Dwivedi, R. Prasad, Recent developments in heterogeneous catalyzed epoxidation of styrene to styrene oxide, *ChemistrySelect* 4 (40) (2019) 11636–11673.
[3] K. Miyamoto, K. Okuro, H. Ohta, Substrate specificity and reaction mechanism of recombinant styrene oxide isomerase from Pseudomonas putida S12, *Tetrahedron Lett.* 48 (18) (2017) 3255–3257.
[4] Y. Liu, Y.C. Zhang, J.Q. Zhao, Progress on epoxidation of alkene catalyzed by titanium silicalite-1, *Fine Chem.* 38 (1) (2018) 9–16, 168.
[5] M. Mitra, O. Cusso, S.S. Bhat, M.Z. Sun, M. Cianfanelli, M. Costas, E. Nordlander, Highly enantioselective epoxidation of olefins by H_2O_2 catalyzed by a non-heme Fe(II) catalyst of a chiral tetradentate ligand, *Dalton Trans.* 48 (18) (2019) 6123–6131.
[6] S.S. Wang, G.Y. Yang, Recent advances in polyoxometalate-catalyzed reactions, *Chem. Rev.* 115 (11) (2015) 4893–4962.
[7] K. Kamata, K. Yonehara, Y. Sumida, K. Yamaguchi, S. Hikichi, N. Mizuno, Efficient epoxidation of olefins with ≥99% selectivity and use of hydrogen peroxide, *Science* 300 (5621) (2003) 964–966.
[8] K. Kamata, Y. Nakagawa, K. Yamaguchi, N. Mizuno, Efficient, regioselective epoxidation of dienes with hydrogen peroxide catalyzed by $[\gamma$-$SiW_{10}O_{34}(H_2O)_2]^{4-}$, *J. Catal.* 224 (1) (2004) 224–228.
[9] W.B. Cunningham, J.D. Tibbetts, M. Hutchby, K.A. Maltby, M.G. Davidson, U. Hintermair, P. Plucinski, S.D. Bull, Sustainable catalytic protocols for the solvent free epoxidation and anti-dihydroxylation of the alkene bonds of biorenewable terpene feedstocks using H_2O_2 as oxidant, *Green Chem.* 22 (2) (2020) 513–524.
[10] S.S. Balula, I.C.M.S. Santos, L. Cunha-Silva, A.P. Carvalho, J. Pires, C. Freire, J.A.S. Cavaleiro, B. de Castro, A.M.V. Cavaleiro, Phosphotungstates as catalysts for monoterpenes oxidation: Homo- and heterogeneous performance, *Catal. Today* 203 (2013) 95–102.
[11] Y.X. Song, F. Xin, L.X. Zhang, Y. Wang, Oxidation of cyclohexene in the presence of transition-metal-substituted phosphotungstates and hydrogen peroxide: Catalysis and reaction pathways, *ChemCatChem* 9 (21) (2017) 4139–4147.
[12] K. Kamata, S. Kuzuya, K. Uehara, S. Yamaguchi, N. Mizuno, μ–η_1:η_1-peroxo-bridged dinuclear peroxotungstate catalytically active for epoxidation of olefins, *Inorg. Chem.* 46 (9) (2007) 3768–3774.
[13] B. Wang, J. Zhang, X. Zou, H.G. Dong, P.J. Yao, Selective oxidation of styrene to 1,2-epoxyethylbenzene by hydrogen peroxide over heterogeneous phosphomolybdic acid supported on ionic liquid modified MCM–41, *Chem. Eng. J.* 260 (2015) 172–177.
[14] X.X. Zhao, J.H. Sun, G.X. Sun, Q. You, X.C. Jiang, Y. Cui, Epoxidation of allyl chloride with H_2O_2 catalyzed by three structurally related quaternary ammonium modified polyoxophosphotungstates, *Appl. Catal. A: Gen.* 608 (2020) 117846.
[15] J.H. Sun, X.X. Zhao, G.X. Sun, S. Zeb, Y. Cui, Q. You, Thermodynamic and kinetic study on the catalytic epoxidation of allyl chloride with H_2O_2 by new catalyst $[(C_{18}H_{37})_2(CH_3)_2N]_3\{PO_4\ W(O)(O_2)_2\}_4\}$, *Chem. Eng. J.* 398 (2020) 125051.
[16] Y. Kon, H. Hachiya, Y. Ono, T. Matsumoto, K. Sato, An effective synthesis of acid-sensitive epoxides *via* oxidation of terpenes and styrenes using hydrogen peroxide under organic solvent-free conditions, *Synthesis* 7 (2011) 1092–1098.
[17] S. Omwoma, C.T. Gore, Y.C. Ji, C.W. Hu, Y.F. Song, Environmentally benign polyoxometalate materials, *Coord. Chem. Rev.* 286 (2015) 17–29.
[18] Y.L. Luo, C.J. Liu, H.R. Yue, S.Y. Tang, Y.M. Zhu, B. Liang, Selective oxidation of cyclopentene with H_2O_2 by using $H_3PW_{12}O_{40}$ and TBAB as a phase transfer catalyst, *Chin. J. Chem. Eng.* 27 (8) (2019) 1851–1856.
[19] A. Dolbecq, E. Dumas, C.R. Mayer, P. Mialane, Hybrid organic−inorganic polyoxometalate compounds: From structural diversity to applications, *Chem. Rev.* 110 (10) (2010) 6009–6048.
[20] Y. Nakagawa, K. Uehara, N. Mizuno, Reactivity of bis(mu-hydroxo) divanadium site in γ-$H_2SiV_2W_{10}O_{40}^{4-}$ with hydroxo compounds, *Inorg. Chem.* 44 (24) (2005) 9068–9075.
[21] Y. Zhou, Z.J. Guo, W. Hou, Q. Wang, J. Wang, Polyoxometalate-based phase transfer catalysis for liquid-solid organic reactions: A review, *Catal. Sci. Technol.* 5 (9) (2015) 4324–4335.
[22] W. Zhao, Y. Ding, Z.X. Zhang, B.C. Ma, W.Y. Qiu, $[(C_{18}H_{37})_2(CH_3)_2N]_7[PW_{11}O_{39}]$: A temperature-controlled phase transfer catalyst for olefin epoxidation, *React. Kinet. Mech. Catal.* 102 (1) (2011) 93–102.
[23] H. Hachiya, Y. Kon, Y. Ono, K. Takumi, N. Sasagawa, Y. Ezaki, K. Sato, Unique salt effect on the high yield synthesis of acid-labile terpene oxides using hydrogen peroxide under acidic aqueous conditions, *Synlett* 19 (2011) 2819–2822.
[24] M.F.M.G. Resul, A.M.L. Fernandez, A. Rehman, A.P. Harvey, Development of a selective, solvent-free epoxidation of limonene using hydrogen peroxide and a tungsten-based catalyst, *React. Chem. Eng.* 3 (5) (2018) 747–756.
[25] S. Pathan, A. Patel, Novel heterogeneous catalyst, supported undecamolybdophosphate: Synthesis, physico–chemical characterization and solvent-free oxidation of styrene, *Dalton Trans.* 40 (2) (2011) 348–355.
[26] A. Patel, R. Sadasivan, Hybrid catalyst based on Cu substituted phosphotungstate and imidazole: Synthesis, spectroscopic characterization, solvent free oxidation of styrene with TBHP and kinetics, *Catal. Lett.* 150 (2) (2020) 353–364.
[27] R. Sadasivan, A. Patel, Flexible oxidation of styrene using TBHP over zirconia supported mono-copper substituted phosphotungstate, *RSC Adv.* 9 (48) (2019) 27755–27767.
[28] R. Sadasivan, A. Patel, A. Ballabh, Investigation of catalytic properties of Cs salt of di-copper substituted phosphotungstate, $Cs_7[PW_{10}Cu_2(H_2O)O_{38}]$ in epoxidation of styrene, *Inorg. Chim. Acta* 487 (2019) 345–353.
[29] S. Keshipour, M. Khezerloo, Gold nanoparticles supported on cellulose aerogel as a new efficient catalyst for epoxidation of styrene, *J. Iran. Chem. Soc.* 14 (5) (2017) 1107–1112.
[30] P.J. Domaille, Vanadium(V) substituted dodecatungstophosphates, *Inorg. Synth.* 29 (1990) 96–104.
[31] S. Singh, A. Patel, Mono lacunary phosphotungstate anchored to MCM–41 as recyclable catalyst for biodiesel production *via* transesterification of waste cooking oil, *Fuel* 159 (2015) 720–727.
[32] C. Venturello, R. Daloisio, Quaternary ammonium tetrakis (diperoxotungsto) phosphates(3^-) as a new class of catalyst for efficient alkene epoxidation with hydrogen peroxide, *J. Org. Chem.* 53 (7) (1988) 1553–1557.
[33] D.C. Duncan, R.C. Chambers, E. Hecht, C.L. Hill, Mechanism and dynamics in the $H_3[PW_{12}O_{40}]$-catalyzed selective epoxidation of terminal olefins by H_2O_2. formation, reactivity, and stability of $\{PO_4[WO(O_2)_2]_4\}^3$, *J. Am. Chem. Soc.* 117 (2) (1995) 681–691.
[34] Y.Y. Chen, J.Q. Zhuang, X.M. Liu, J.B. Gao, X.W. Han, X.H. Bao, N. Zhou, S. Gao, Z. W. Xi, On the nature of reaction-controlled phase transfer catalysts for

epoxidation of olefin: A ^{31}P NMR investigation, *Catal. Lett.* 93 (1–2) (2004) 41–46.
[35] T. Okuhara, M. Mizuno, M. Misono, Catalytic chemistry of heteropoly compounds, *Adv. Catal.* 41 (1996) 113–252.
[36] A.M. Hyde, S.L. Zultanski, J.H. Waldman, Y.L. Zhong, M. Shevlin, F. Peng, General principles and strategies for salting-out informed by the hofmeister series, *Org. Process Res. Dev.* 21 (9) (2017) 1355–1370.
[37] J.Y.Z. Zhang, Y.D. Wang, G.W. Stevens, W.Y. Fei, An experimental study on single drop rising in a low interfacial tension liquid–liquid system, *Chem. Eng. Res. Des.* 148 (2019) 349–360.
[38] T.A.G. Duarte, A.C. Estrada, M.M.Q. Simoes, I.C.M.S. Santos, A.M.V. Cavaleiro, M. G.P.M.S. Neves, J.A.S. Cavaleiro, Homogeneous catalytic oxidation of styrene and styrene derivatives with hydrogen peroxide in the presence of transition metal-substituted polyoxotungstates, *Catal. Sci. Technol.* 5 (1) (2015) 351–363.
[39] W.Q. Yuan, S.Q. Zhou, Y.Y. Jiang, H.H. Li, H.D. Zheng, Organocatalyzed styrene epoxidation accelerated by continuous-flow reactor, *J. Flow Chem.* 10 (1) (2020) 227–234.
[40] O.A. Kholdeeva, O.V. Zalomaeva, Recent advances in transition-metal-catalyzed selective oxidation of substituted phenols and methoxyarenes with environmentally benign oxidants, *Coord. Chem. Rev.* 306 (2016) 302–330.
[41] H. Taghiyar, B. Yadollahi, New perspective to catalytic epoxidation of olefins by Keplerate containing Keggin polyoxometalates, *Polyhedron* 156 (2018) 98–104.
[42] Y. Lu, X. Zhang, X.B. Cui, J.Q. Xu, A series of compounds based on $[P_2W_{18}O_{62}]^{6-}$ and transition metal mixed organic ligand complexes with high catalytic properties for styrene epoxidation, *Inorg. Chem.* 57 (17) (2018) 11123–11134.
[43] Z.L. Shi, C.Z. Mei, G.Q. Niu, Q.X. Han, Two inorganic-organic hybrids based on a polyoxometalate: Structures, characterizations, and epoxidation of olefins, *J. Coord. Chem.* 71 (9) (2018) 1460–1468.
[44] A. Hachemaoui, A. Yahiaoui, M. Belbachir, Structural and photooxidation studies of poly(styrene oxide) prepared with maghnite-H^+ as cationic catalyst, *J. Appl. Polym. Sci.* 110 (5) (2008) 3195–3202.
[45] H. Misaka, R. Sakai, T. Satoh, T. Kakuchi, Synthesis of high molecular weight and end-functionalized poly(styrene oxide) by living ring-opening polymerization of styrene oxide using the alcohol/phosphazene base initiating system, *Macromolecules* 44 (23) (2011) 9099–9107.
[46] A. Yahiaoui, M. Belbachir, J.C. Soutif, L. Fontaine, Synthesis and structural analyses of poly (1,2-cyclohexene oxide) over solid acid catalyst, *Mater. Lett.* 59 (7) (2005) 759–767.